Nonergodic Arrested State in Diluted Clay Suspensions Monitored by Triple-Quantum ^{23}Na Nuclear Magnetic Resonance

T. Gili,* S. Capuani, and B. Maraviglia

CNR-INFM CRS-SOFT, Universitá di Roma "La Sapienza",P.zle A. Moro 5, I-00185 Roma, Italy, Dipartimento di Fisica, Universitá di Roma "La Sapienza", P.zle A. Moro 5, I-00185 Roma, Italy, Enrico Fermi Center, Compendio Viminale, I-00184 Roma, Italy, and Fondaziona Santa Lucia IRCCS, I-00179 Roma, Italy

Received: January 22, 2007; In Final Form: March 30, 2007

The aging of water suspension of the synthetic clay Laponite has been studied by liquid-state triple-quantum filter nuclear magnetic resonance techniques, in a range of clay weight concentration ($C_w = 0.012-0.028$) known as the isotropic phase. Counterions dynamic parameters (rotational correlation time τ_c and quadrupolar coupling constant e^2qQ/h) have been extracted from sodium triple-quantum filtered experimental data within the multi-exponential quadrupolar relaxation theory in the fast exchange approximation. By monitoring quadrupolar sodium ions dynamical (τ_c and e^2qQ/h) and static (counterion concentration p_b) properties during the aging, we find two different mechanisms of transition toward an arrested state. Our experimental findings match with the description which states, at low concentration, the formation of clusters of Laponite disks trigger the reaching of the arrested state, while at high concentration, single disks are the basic units of the arrested phase. The procedure proposed in this paper, based on multiple quantum filtered NMR data analysis, results to be a useful means to study the routes to arrested states in aqueous colloidal dispersions.

Introduction

In recent years the analogies between colloidal glasses and gels have stimulated an increased effort, to unify the description of the transitions toward these disordered jammed states[1,2] of soft condensed matter within a single conceptual framework. Whenever short-ranged attractive interactions are complemented by weak repulsive electrostatic interactions, the gel formation process can be fully modeled as a glass transition phenomenon.[3]

Suspensions of charged lamellae has been the subject of several experimental investigations,[4] showing the relationship between structural and mechanical properties of these strongly coupled systems. In spite of this intensive research, there is no general agreement about the mechanism that initiates the arrested phases in Laponite suspensions, attributed by different authors to Wigner glass transition, frustrated nematic transition, gelation, etc. Phase diagrams of charged anisotropic colloidal particles suspensions have been proposed,[5,6] attempting to define the nature of the nonergodic disordered state shown by these systems. As indicated in recent works[6,7] a parallelism may be recognized between the reentrant phase of ref 3 and the phase diagram of a synthetic Hectorite clay: Laponite.

According to the phase diagram,[5] at ionic strength below $I = 10^{-2}$ M and at concentrations below $C_w = 3\%$, diluted Laponite suspensions can be in two different physical states. Low concentration suspensions [$C_w < C_w^*(I)$] (isotropic liquid phase) form a stable, equilibrium fluid phase. Higher concentration suspensions [$C_w \gtrsim C_w^*(I)$] (isotropic gel phase) are initially fluids but experience aging and pass into a gel phase after a time that depends on the clay amount. Recently, an unexpected arrested phase has been observed in low concentration suspensions, and it has been attributed to glass transition by different authors.[7−10]

* To whom correspondence should be addressed. Phone: 390649913928. E-mail: tommaso.gili@romal.infn.it.

Nuclear Magnetic Resonance (NMR) studies of aging of high concentration Laponite suspensions have been realized in recent years.[11−13] We present here a ^{23}Na (nuclear spin $S = 3/2$) liquid-state NMR triple-quantum filtered spectroscopic study of Laponite suspensions in the concentration range (1.2−2.8%), at ionic strength $I = 10^{-4}$ M. We demonstrate that sodium ions dynamic parameters (such as rotational correlation time τ_c and quadrupolar coupling constant QCC), in low concentration Laponite suspensions, may be achieved by means of ^{23}Na triple-quantum filters NMR techniques.[14−16] In all Laponite aqueous suspensions, sodium ions are considered attending two dynamical regions: the bulk region and the electrostatic screening shell around each charged disk (Figure 1). In the bulk, the ions experience a dynamical state characterized by a correlation time much shorter than the inverse of the Larmor frequency ω_0, while in the electrostatic screening shell, due to the quadrupolar interaction with the charged surfaces of the Laponite disk,[17] the ions experience an $\omega_0\tau_c \gtrsim 1$ dynamical state. Adsorbed counterions (Stern layer) are not taken into account, because they are not detectable by means of liquid-state NMR spectroscopy. We show that the monitoring of the bound counterions (the ions attending the electrostatic screening shells) concentration p_b of τ_c and QCC provides an original way to follow aging dynamics of low-density charged disk-like colloidal particles. Here we confirm the aging process of samples belonging to a low concentration phase region and we provide information about p_b variation during the aging. Furthermore, based on our NMR results, we describe two different mechanisms of transition toward Laponite suspension arrested states as a function of disks concentration.

Theoretical Background

Sodium Multi-relaxation And Triple-Quantum Signal. NMR behavior of spin $S = 3/2$ nuclei in soft condensed matter is dominated by the quadrupolar interaction. In the absence of

10.1021/jp070533v CCC: $37.00
Published on Web 05/31/2007

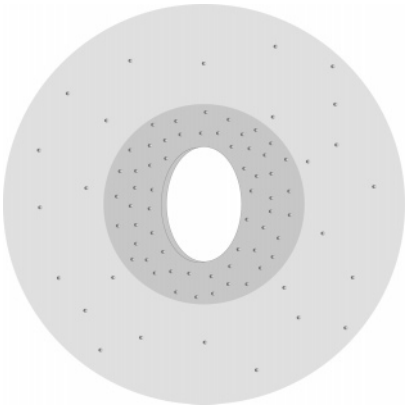

Figure 1. Sodium ions (black spheres) dynamical regions depicted in two different gray levels. Light gray region: the bulk region of sodium ions involved in $\omega_0\tau_c \ll 1$ dynamical state; dark gray region: electrostatic screening shell of sodium ions around Laponite charged platelet (white disk), in which ^{23}Na nuclei are involved in $\omega_0\tau_c \gtrsim 1$ dynamical state. Here, the ^{23}Na ions in $\omega_0\tau_c \gtrsim 1$ dynamical state are named bound counterions. Adsorbed counterions are not taken into account.

quadrupolar splittings, i.e., if the quadrupolar interaction is averaged to zero, $\langle\omega_q\rangle = 0$, three degenerate single quantum transitions (transitions with $\Delta m = \pm 1$, where m is the magnetic quantum number) are allowed. The interaction between the nuclear quadrupole moment (Q_{ij}) and the local electric field gradient (EFG) leads to a perturbation of the energy levels. When the electric field gradients fluctuate in time, two distinct situations may occur. If the fluctuation is fast, so that its own correlation time is short compared with the Larmor period of the nucleus ($\omega_0\tau_c \ll 1$, where ω_0 is the Larmor frequency), longitudinal and transverse relaxations are monoexponential, a situation known as extreme narrowing limit. Vice versa if the correlation time is long compared with the Larmor period of the nucleus ($\omega_0\tau_c \gtrsim 1$), the relaxation is multiexponential.[14,18,19] Thus, if the nuclei under investigation are associated with macromolecules, clusters, or slowly tumbling complexes, the relaxation is multiexponential. The detection of triple-quantum coherences of $S = 3/2$ spins provides a straightforward measure of dynamical parameters (τ_c and QCC) related to those spins satisfying the condition $\omega_0\tau_c \gtrsim 1$.[14,15] In other words, by means of triple-quantum filtered sequences, it is possible to obtain a signal exclusively from sodium nuclei which are involved in coulombian screening shells around charged Laponite disks (bound counterions p_b).

In the following, we describe spin dynamics by means of density matrix evolution formalism.[20] A coherence can be associated with a transition between two states. If the difference in the magnetic quantum number of the two states is $\Delta m = \pm 1$, the coherence is related to transverse observable magnetization. If $\Delta m = \pm p$ ($p \neq 1$), the p-quantum coherence does not lead to observable magnetization and it can be detected only indirectly. In the absence of quadrupolar splittings, the excitation and observation of multiple-quantum coherences are made possible by multiexponential relaxation, in a manner that is related to violations of coherence transfer selection rules observed for equivalent protons in methyl groups (group spin $S = 3/2$).[21] An rf pulse sequence that perturbs the equilibrium density matrix, creating transitions with $\Delta m \neq \pm 1$, and then converts the multiple-quantum coherences into observable signal (transversal magnetization) is called a multiple-quantum filter. In the theoretical description of quadrupolar spins, under triple-quantum filtering rf pulse sequences, the density matrix is conveniently written in terms of irreducible tensor operators.[14] Thermal equilibrium at high field is described by a tensor $T_{1,0}$ of first rank and zeroth order ("Zeeman order"). This can be transformed into coherence of first rank and first-order $T_{1,\pm1}$ (single quantum coherence) by a 90° rf pulse. Rf pulse can change the coherence order, while the evolution under the quadrupolar interaction or relaxation mechanisms can alter the rank of a coherence. Free evolution of $S = 3/2$ spins under the quadrupolar interaction can lead to the transformation of $T_{1,\pm1}$ coherence into second and third rank terms, $T_{2,\pm1}$ and $T_{3,\pm1}$. The effect of electrostatic screening capture on ^{23}Na, and the related correlation time τ_c increase, can be monitored by tracking the $T_{3,\pm1}$ coherences. This requires a sequence of four rf pulses, named triple-quantum filtered spin echo (TQFse):[14]

$$[90° - \tau - 180° - \tau - 90°_{\phi'}]_{\phi} - \tau_m - 90° - \text{acquisition} \quad (1)$$

where the phase ϕ is cycled through {0°, 60°, 120°, 180°, 240°, 300°} to retain triple-quantum coherences, while the receiver phase is alternated. The fixed relative phase ϕ' must be set to 90° for triple-quantum filters (TQF). The initial 90° pulse generates first-rank single-quantum coherence, $T_{1,\pm1}$. During the interval 2τ, second- and third-rank single quantum coherences, $T_{2,\pm1}$ and $T_{3,\pm1}$, can be created due to quadrupolar relaxation. However, because of the lack of the quadrupolar splitting second rank terms are not created. The 180° pulse allows one to refocus offset effects. In the brief interval τ_m (typically a few microseconds to allow the transmitter phase to be shifted), the transverse magnetization is temporarily converted into third-rank double- and triple-quantum coherences, $T_{3,\pm2}$ and $T_{3,\pm3}$. After the cancellation of all terms other than the desired triple-quantum coherences (by an appropriate phase cycle), $T_{3,\pm2}$ and $T_{3,\pm3}$ coherences are converted back into $T_{3,\pm1}$ by the last pulse. Although the latter term is not directly observable, it can be reconverted through further quadrupolar relaxation processes into observable $T_{1,\pm1}$. This first-rank single-quantum coherence can be detected by the receiver, which is activated immediately after the last pulse. As a consequence, the signal acquired is a double exponential function of τ (Figure 2b):

$$I^{(1)}(\tau) = I_0^{(1)}\{\exp[-R_1^{(1)}\tau] - \exp[-R_2^{(1)}\tau]\} \quad (2)$$

The fast and slow transverse relaxation rates, $R_1^{(1)}$ and $R_2^{(1)}$, are defined as $R_1^{(1)} = C(J_0 + J_1)$ and $R_2^{(1)} = C(J_1 + J_2)$, being $C = (e^2qQ/\hbar)^2/40$ and $J_n = 2\tau_c/[1 + (n\omega_0\tau_c)^2]$.

It is also possible to probe the multiexponential character of longitudinal relaxation performing triple-quantum filtered inversion recovery experiments (TQFir):[14]

$$180° - \tau - 90°_{\phi} - \tau_m - 90° - \text{acquisition} \quad (3)$$

Quadrupolar relaxation in the τ interval lead to the conversion of inverted Zeeman order -$T_{1,0}$ into (third-rank) octupolar order $T_{3,0}$, which may be temporarily converted by the second pulse into third-rank double- and triple-quantum coherences $T_{3,\pm2}$ and $T_{3,\pm3}$, and subsequently into observable coherence $T_{1,\pm1}$. TQFir experiments were at least an order of magnitude weaker than those observed with the echo sequence of eq 1. The signal trend at the end of the sequence eq 3 is a double exponential function of τ (Figure 2a):

$$I^{(0)}(\tau) = I_0^{(0)}\{\exp[-R_1^{(0)}\tau] - \exp[-R_2^{(0)}\tau]\} \quad (4)$$

The slow and fast longitudinal relaxation rates, $R_1^{(0)}$ and $R_2^{(0)}$, are defined as $R_1^{(0)} = 2CJ_1$ and $R_2^{(0)} = 2CJ_2$.

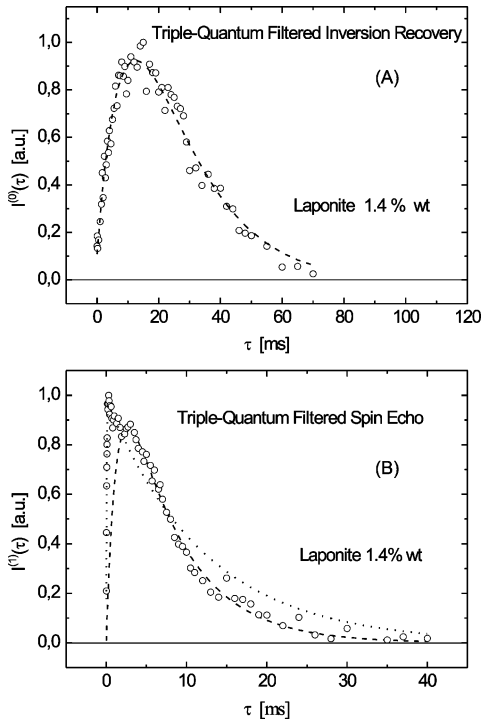

Figure 2. Triple-quantum filtered inversion recovery (A) and spin echo (B) experimental data. The dotted and dashed lines are the results of Levenberg−Marquardt fitting procedures based on the functions described in the text. Relaxation rates extracted from fits are as follows: (A) $R_1^{(0)} = (64 \pm 1)s^{-1}$, $R_2^{(0)} = (67 \pm 1)s^{-1}$; (B) $R_1^{(1)} = (82 \pm 1)s^{-1}$, $R_2^{(1)} = (20 \pm 1)10^3\ s^{-1}$ (first double exponential trend) and $R_1^{(1)} = (142 \pm 5)s^{-1}$, $R_2^{(1)} = (779 \pm 60)s^{-1}$ (second double exponential trend). The confidence level in figure (B) is given by $R^2 = 0.983$ for the first double exponential curve and by $R^2 = 0.991$ for the second one, being the two curves fitted separately; if one would fit the entire trend with a single double exponential it would be obtained $R^2 = 0.697$.

Experimental Section

Materials. Laponite suspensions are composed of monodisperse, rigid, disc-shaped platelets with a thickness of 1 nm and a diameter of about 30 nm. A single disk is composed by nearly 1500 unit cells each of which is a trioctahedral clay, obtained by sandwiching one layer of octahedral magnesium oxide between two layers of tetrahedral silicium oxide both of them carrying a sodium ion. The negative surface charge is due to sodium counterions release in water solution, while the positive charge of the lateral rim is a consequence of the substitution of some magnesium cations of the octahedral layer by lithium cations.

Six Laponite (Laporte Ltd.) aqueous suspensions, at the desired weight concentrations of 1.2, 1.4, 1.7, 2.0, 2.4, and 2.8 wt %, were investigated. Particular attention has been given to sample preparation to avoid the observed degradation or dissolution of Laponite particles in the presence of atmospheric CO_2.[22,23] For this reason the whole preparation procedure has been performed in a glove box under N_2 flux and the samples have been always kept in safe atmosphere during and after sample preparation. The powder was dispersed in deionized (pH 7) water and D_2O (volume ratio H_2O:D_2O = 3:1), stirred vigorously until the suspensions were cleared, filtered through 0.45 μm pore size Millipore filters and then sealed in quartz NMR tube. The starting aging time ($t_w = 0$) is defined as the time when the suspension is filtered. This sample preparation procedure is similar to that already used in previous works.[24,25]

NMR Measurements. NMR measurements were performed using a Bruker Avance 400 system in combination with a 9.4T superconducting ultrashield magnet. The probe used was a 5 mm multinuclear (e.g., ^{109}Ag to ^{31}P in one range plus ^{1}H) high-resolution broad band observe (BBO). Samples temperature was controlled by means of Bruker BVT 3200 system, a thermocouple based remote control system, and it was fixed at T = 298 K. We performed NMR measurements on ^{23}Na nuclei (ν_0 = 105.8 MHz at B_0 = 9.4 T) in Laponite samples. Lorentzian line obtained after Fourier transformation of the free induction decay (FID) has a full width at half-maximum ~60 Hz, and it is characterized by the lack of quadrupolar splitting in each experiment. In both TQFse and TQFir the number of signal averages NS = 1536, the aquisition time AQ = 20 ms, the mixing time $\tau_m = 5$ μs and the repetition time TR = 95 ms were set. The phase cycling used to retain triple-quantum coherences was enriched with π-cycles over each pulse to correct the rf pulse imperfections. The drift of the static magnetic field was controlled by means of a lock engine set on the deuterium signal.

Data Analysis. TQFse and TQFir experimental data (Figure 2) were both analyzed by means of Levenberg−Marquardt fitting procedures on the basis of eq 2 and eq 4 respectively. We observed a clear difference between TQFse and the TQFir trends: longitudinal relaxation rates ($R_1^{(0)}$,$R_2^{(0)}$) are roughly equal within the errors in all of the experiments we performed, while transverse relaxation rates ($R_1^{(1)}$, $R_2^{(1)}$) substantially differ one respect with the other (Figure 2). Moreover the distinction between Isotropic Gel region ($C_w \leq C_w^*$) and Isotropic Liquid region ($C_w > C_w^*$) maight be identified in the TQFse trends behavior. In fact, if on one hand, TQFse experimental data of C_w = 2.0−2.8% are distributed as a pure double exponential function, on the other hand $C_w < 2.0\%$ Laponite concentrations show a superposition of two distinguishable double exponential functions (Figures 2b and 3a). To test the effectiveness of this statement, we compared two kinds of fitting procedures of *TQ*Fse data, one on the basis of two double exponential functions fitted separately, and the other on the basis of a single-exponential function (Figure 2). In the first case we found two independent regression fidelity levels R^2 both equal to 98−99%, one for each double exponential (Figure 2b), while in the second case, it was found that R^2 is equal to 70%. For this reason we analyzed $C_w < 2.0\%$ experimental data by means of two independent double exponential fitting functions, extracting τ_c and e^2qQ/h for both of the signal trends. As time flowed, the disappearance of the second superimposed double exponential trend in $C_w \leq C_w^*$ suspensions *TQ*Fse signal behavior has been observed (Figure 3b), suggesting the existence of an aging phenomenon, as it was indicated in ref 7, and reducing to a single double exponential that used the fitting function. The results of the fitting procedure on TQFir experimental data show the lack of sufficient precision to distinguish the two relaxation rates, suggesting the chance to evaluate the mean value of the triple-quantum filtered longitudinal relaxation time $\langle T_1 \rangle_{TQFir}$ as the inverse of the mean of $R_1^{(0)}$ and $R_2^{(0)}$.

Results and Discussion

Relative Counterions Concentration. The relative amount of the sodium ions involved in electrostatic screening shells around charged Laponite platelets (bound counterions) has been obtained by TQFir experimental data. A roughly constant signal trend characterized by fast and slow relaxation times ($T_1^{fast} = 1/R_2^{(0)}$, $T_1^{slow} = 1/R_1^{(0)}$), during the aging, suggests a poor sensitivity of these parameters to dynamical changes in our samples. Nonetheless, variations in standard inversion recovery (IR)

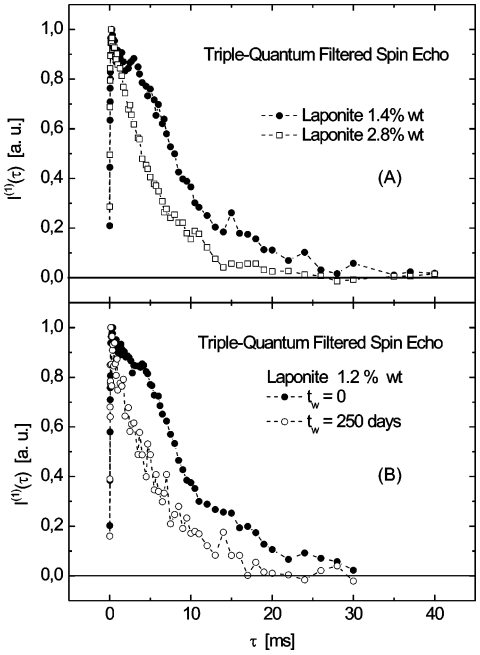

Figure 3. Triple-quantum filtered spin echo experimental data: (a) the comparison between $C_w = 1.4\%$ and $C_w = 2.8\%$ signal amplitude trends detected at waiting time $t_w = 0$; (b) the comparison between $C_w = 1.2\%$ signal amplitude trends at $t_w = 0$ and at $t_w = 250$ days. The dashed lines are drawn to guide eye only.

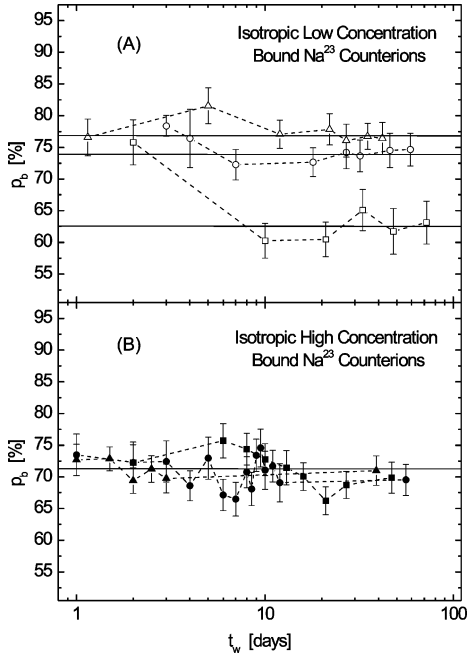

Figure 4. Bound counterions variations during the aging. (A) Isotropic low concentration (ILC): (□) 1.2 wt %, (○) 1.4 wt %, (△) 1.7 wt %; (B) Isotropic high concentration (IHC): (■) 2.0 wt %, (●) 2.4 wt %, (▲) 2.8 wt %. The solid lines represent the p_b asymptotic values reached at long waiting time t_w. The dashed lines are drawn to guide eye only.

experiments may be observed,[26] which involve the entire population of ^{23}Na nuclei in the sample. As a consequence, since the signal detected in TQFir experiments comes only from those nuclei marked by the $\omega_0\tau_c \gtrsim 1$ dynamical condition, the variations observed must be due to changes in relative populations living in the two different dynamical states. Due to fast exchange processes[27] it may be distinguished between the free ^{23}Na population fraction p_f and the bound ^{23}Na population fraction p_b; thus, the contribution to inversion recovery relaxation time (T_1^{IR}) runs it follows: $(1/T_1)_{IR} = p_f(1/T_1)_{bulk} + p_b(1/\langle T_1\rangle)_{TQFir}$, where $\langle T_1\rangle$ is the mean value of T_1^{slow} and T_1^{fast}. Since $p_f + p_b = 1$, the bound counterions concentration is given by the following:

$$p_b = \frac{\left(\frac{1}{T_1}\right)_{IR} - \left(\frac{1}{T_1}\right)_{bulk}}{\left(\frac{1}{\langle T_1\rangle}\right)_{TQFir} - \left(\frac{1}{T_1}\right)_{bulk}} \qquad (5)$$

Distinction between two dynamical regions may be done: the bulk region and the electrostatic screening region of Laponite charged disks (Figure 1). In fact the electric field gradient fluctuations, responsible for quadrupolar relaxation of ^{23}Na nuclei with $\omega_0\tau_c \gtrsim 1$, come from charge fluctuations on Laponite surfaces; as a consequence the so-called bound counterions are the nuclei attending the Debye screening shell.[17] Adsorbed counterions (Stern layer) are not taken into account, because their presence would be mirrored in a quadrupolar splitting of the spectrum which we never detect. Isotropic high concentrations (IHC) $C_w \geq 2.0\%$ exhibit a common constant trend around $p_b = 70\%$ for long waiting time t_w (Figure 4b). On the other hand, an early aging time may be defined as the initial period of not screening length stability, which is mirrored in a decreasing behavior of p_b trend down to an asymptotic value. The starting point of this decreasing trends may be recognized in $p_b = 76, 77, 80\%$ for $C_w = 2.8, 2.4, 2.0\%$ respectively; besides, the lower the sample concentration the slower the decreasing rate. Isotropic low concentration (ILC) samples $C_w < 2.0\%$ are characterized by a different behavior. In fact, if on one hand a decrease marks all samples reported in early aging, on the other hand the constant trend achieved at long waiting scales as a concave function with sample concentration. We may recognize an increasing asymptotic value when Laponite concentration increases up to $C_w = 1.7\%$, then the asymptote decreases down to a lower value for $C_w = 2.0\%$ (Figure 4a). This findings suggest that the screening length decreases when the sample concentration increases, up to $C_w = 2.0\%$, when a jump to a lower screening length is exhibited, as the system would fall in a more stable configuration. At very long waiting time $C_w = 1.7\%$ exhibits one more decrease reaching the same asymptotic value got by $C_w = 2.0\%$.

Dynamical properties of the sodium counterions, involved in electrostatic screening shells around Laponite disks, have been studied by means of *TQ*se experiments monitoring the aging of the six Laponite suspensions prepared. IHC and ILC show a typical double exponential decay as predicted by theory. However, if one looks at slow component of Triple-quantum filtered transverse relaxation times a substantial distinction rises. The comparison of the two triple-quantum curves reported in Figure 3 reveals the existence of an additional relaxation process. Despite of a substantial equality of both signals increasing during short delay time, the decreasing trend of slow relaxation components clearly exhibit two different relaxation paths: $C_w = 2.8\%$ follows the double exponential trend predicted by theory; $C_w = 1.4\%$ shows the presence of two relaxation mechanisms of $^{+}$Na, which mirror themselves into a second double exponential trend peeping out of the expected trend. The invariance in chemical properties of ^{23}Na (highlighted by the line shape analysis all along the aging process) and the absence of double-quantum signal contamination[26] suggested that more than one bound ^{23}Na dynamical state ought to be invoked to explain this signal trend anomaly. No dynamical exchange between $^{+}$Na($\omega_0\tau_c \gtrsim 1$) and $^{+}$Na($\omega_0\tau_c \ll 1$) may affect NMR

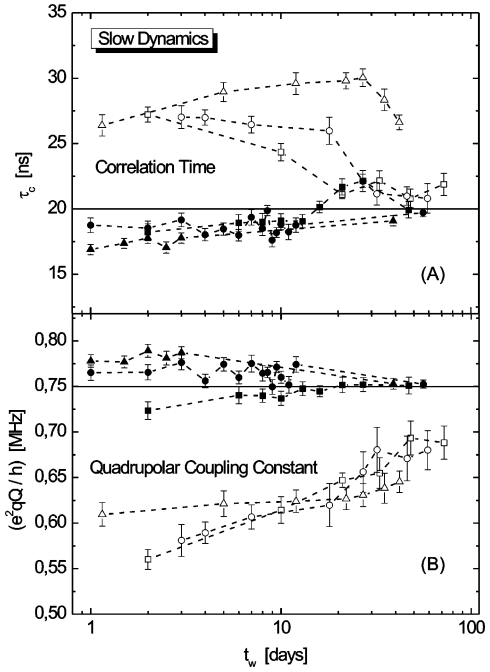

Figure 5. Slow Dynamics parameters as a function of the aging time at the temperature of 298 K for different sample concentrations: (□) 1.2 wt %, (○) 1.4 wt %, (△) 1.7 wt %, (■) 2.0 wt %, (●) 2.4 wt %, (▲) 2.8 wt %. (A) Correlation time; (B) Quadrupolar coupling constant. The solid lines represent asymptotic values reached by dynamical parameters of the different samples at long waiting time t_w; the dashed lines are drawn to guide eye only.

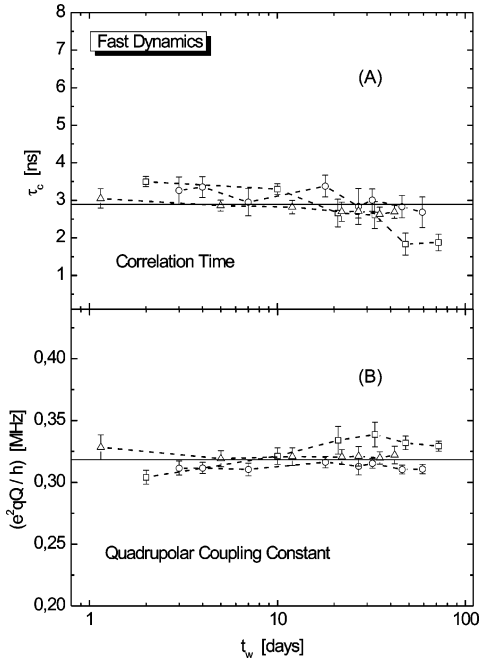

Figure 6. Fast dynamics parameters as a function of the aging time at the temperature of 298 K for different sample concentrations: (□) 1.2 wt %, (○) 1.4 wt %, (△) 1.7 wt %. (A) Correlation time; (B) Quadrupolar coupling constant. The solid lines represent asymptotic values reached by dynamical parameters of the different samples at long waiting time t_w; the dashed lines are drawn to guide eye only.

signal. In fact exchange processes involve either chemical exchange or magnetization changes.[27] The first of them is not to be considered owing to the ionic nature of sodium in solution; the way it interacts with the surrounding environment is via electrostatic interactions, thus no NMR quantities variation due to chemical changes can be detected. However, due to fast dynamical exchange limit of sodium in solution, also magnetization density changes cannot be taken into account: the amount of $^{+}\mathrm{Na}(\omega_0\tau_c \ll 1)$ which migrate in free counterions region is the same of $^{+}\mathrm{Na}(\omega_0\tau_c \gtrsim 1)$ which move in the opposite way; this exchange is so fast that counterions configuration does not vary during an NMR experiment, that is free and bound counterions are frozen in their dynamical states and only relative populations affect experimental results. Thus it is clear the choice to separately fit the two superimposed ILC double exponential trends. In the coalescence of the two curves, we noticed that the first trend persists all along the aging, while the second exhibits a changeable behavior.

In fact, as it is reported in Figure 3, the coalescence of the two curves, corresponding to the two dynamical states (both $(\omega_0\tau_c \gtrsim 1)$ kind), changes during the aging. $C_w = 1.2\%$ exhibits a regress of coalescence as far as a collapse into only one double exponential trend is achieved (Figure 3a). This findings suggest that $^{+}\mathrm{Na}(\omega_0\tau_c \gtrsim 1)$ in ILC Laponite samples feel, during the aging, a double electric field gradient fluctuating environment: the first one, related to the first double exponential trend, is due to single disk fluctuations; the other, related to the second superimposed double exponenial, is due to collective disks fluctuations.

Rotational Correlation Time and Quadrupolar Coupling Constant. The interpretation of dynamical experimental results in Figure 5a is straightforward. The main difference in correlation time obtained by means of the two double exponential fits concerns their absolute values, which differ by an order of magnitude. As previously observed, τ_c establishes the time-scale the nuclear system has to wait memory loss of electric field gradient fluctuations due to nuclear rotationts. Thus, the second superimposed trend is related to those fluctuations easy to be forgotten, while, the first one is related to those fluctuations less easy to be forgotten; as a consequence it may be distinguished between slow (first double exponential) and fast (second double exponential) dynamics. As far as the IHC and ILC slow dynamics trends is concerned, immediately two opposite behaviors are glaring. IHC exhibit an increase up to $\tau_c = 19$ ns asymptotic value, while ILC decrease down to $\tau_c = 21$ ns. Besides, $C_w = 1.7\%$ and $C_w = 2.0\%$ are worth making a separate remark. In fact, their trends involve first an increase up to a maximum value, followed by a decrease down to the asymptotic value related to the concentration group they belong to. It can be ascribed to a transition in setup configuration of Laponite disks between IHC and ILC, assisted, as reported in Figure 4, by counterions release. Fast dynamics τ_c behavior, not reported, exhibits a common constant trend for all the concentrations up to its disappearing at long aging times.

As far as QCC is concerned, IHC and ILC distinction may be carried on too. Both groups of concentrations exhibit an increasing slow dynamics trend up to an asymptotic value. However QCC absolute values differ one from the other: slow dynamics IHC trends vary between $(e^2qQ/h) = 0.71$ MHz and $(e^2qQ/h) = 0.79$ MHz, while a variation from $(e^2qQ/h) = 0.54$ MHz to $(e^2qQ/h) = 0.69$ MHz is exhibited by ILC in the same dynamical state (Figure 5b). In both cases the increasing rate scale with concentration. It is worth noticing that ILC achieve the saturation toward the same asymptotic value, while, for IHC, we may distinguish different asymptotes related to different concentrations. Conversely a common constant fast dynamics trend (not reported) is exhibited by all the concentrations up to its disappearing at long aging times. Since QCC gives the order of magnitude of the fluctuating interaction strength, it is not surprising that the evolution of single disk fluctuation intensity (Figure 5b) goes together counterions release (Figure 3): that

is the more is the net charge over disks surfaces the larger is the strength of electric field gradient. Nevertheless the existence of fast dynamics (e^2qQ/h) (together with fast dynamics τ_c) may be sufficiently astonishing. We suggest that ILC bound counterions live in an electrostatic environment due to the sum of the EFG of a single Laponite disk plus the superposition of the EFG from neighboring disks. The space these counterions can span is restricted to the region occupied by the ensemble of disks producing collective disk fluctuation. Thus fast and slow dynamics are related to the electrostatic interaction of $^{+}$Na within disk ensemble region and single disk region respectively. A cluster of Laponite disks will be called the disk ensemble region. Clusters my be considered individual unity which span the entire free volume of the solution. During the aging, clusters dynamics is responsible for mutual collision leading to the formation of larger aggregates, up to the moment when they are so large to be blocked. This configuration is related to the disappearance of fast dynamics. In fact sodium ions are able to jump from a cluster to another feeling different superposition of EFG which average to zero, and feeling only EFG due to single disk fluctuations. HC Laponite samples reach the arrested dynamical state by means of a different path. Counterions release leads the Laponite disks to a screening length similar to the $C_w = 1.2\%$ one, but in a sample containing at least twice the disks concentration. Thus it may be said that such systems occupy the free volume in the sample without passing through cluster aggregation. The argument is that for IHC samples there is not enough free volume to build up clusters of disks. Moreover their net surface charge is such that they organize themselves in order to optimize disk−disk interaction, leading to an isotropic network-like configuration of disks along whose meshes bound counterions migrate. ^{23}Na triple-quantum NMR experimental results and their interpretation proposed in this paper are coherent with results obtained by means of light scattering technique and rheology.[4] The microscopic interaction between Laponite platelets is due to a screened Coulomb interaction that can be modeled by a Yukawa-like repulsion at long distances and a quadrupolar attractive electric term at short distances. The presence of long-range repulsion and short-range attraction interactions resembles that recently proposed to describe the phenomenology of colloidal gels. It has been suggested that gelation, taking place in attractive colloidal suspensions at very low concentration, involves the growth of larger and larger clusters (driven by the short-range attraction).

Conclusion

In this paper we showed the great potential of NMR triple-quantum spectroscopy to study aging dynamics of colloidal suspensions from the point of view of counterions dynamics. As the particular subject analyzed here is concerned, our results show the existence of two different mechanisms of transition toward the arrested state of isotropic water suspension of a Laponite disks. The experimental results obtained from triple-quantum experiments on aging in colloidal systems are thus far, to our knowledge, the only data reported in literature. This work fills in the meager literature about NMR description of aging in soft condensed matter. Our main findings concern the existence of multiple relaxation in triple-quantum filtered spin echo data from Laponite samples at concentrations below the transition isotropic-liquid−isotropic-gel. We reported also static properties of $^{+}$Na counterions involved into the electrostatic screening shell around Laponite disks. We showed that bound counterions concentration, which determine the Laponite disks electrostatic screening length, plays a fundamental role in the differentiation of the route to gelation. In fact the difference we observed in the way to reach the arrested phase could be that at low concentrations the arrested phase is due to the formation of clusters, while at high concentrations, the single Laponite platelets would be the elementary constituent of the entire system.

References and Notes

(1) Liu, A. J.; Nagel, S. R. *Nature* (London) **1998**, *396*, 21.

(2) Trappe, V.; Prasad, V.; Cipelletti, L.; Serge, P. N.; Weitz, D. A. *Nature* (London) **2001**, *411*, 772.

(3) Sciortino, F.; Mossa, S.; Zaccarelli, E.; Tartaglia, P. *Phys. Rev. Lett.* **2004**, *93*, 055701.

(4) Ramsay, J. D. F.; and Lindner, P. *J. Chem. Soc. Faraday Trans.* **1993**, *89*, 4207; Mourchid, A.; Delville, A.; Lambard, J.; LeColier, E.; Levitz, P. *Langmuir* **1995**, *11*, 1942; Pignon, F.; Piau, J.; Magnin, A. *Phys. Rev. Lett.* **1996**, *76*, 4857; Bonn, D.; Kellay, H.; Tanaka, H.; Wegdam, G.; Meunier, J. *Langmuir* **1999**, *15*, 7534; Nicolai, T.; Cocard, S. *Langmuir* **2000**, *16*, 8169; Nicolai, T.; Cocard, S. *Eur. Phys. J. E* **2001**, *244*, 51; Abou, B. *et al. Phys. Rev. E* **2001**, *64*, 021510; Abou, B.; Bonn, D.; Meunier, J. *Phys. Rev. Lett.* **2002**, *89*, 15701; Tanaka, H.; Jabbari-Farouji, S.; Meunier, J.; Bonn, D. *Phys. Rev. E* **2005**, *71*, 021402.

(5) Mourchid, A.; Lecolier, E.; Van Damme, H.; Levitz, P. *Langmuir* **1998**, *14*, 4718.

(6) Tanaka, H.; Meunier, J.; Bonn, D. *Phys. Rev. E* **2004**, *69*, 031404.

(7) Ruzicka, B.; Zulian, L.; Ruocco, G. *Phys. Rev. Lett.* **2004**, *93*, 258301.

(8) Bonn, D.; Kellay, H.; Tanaka, H.; Wegdam, G.; Meunier, J. *Langmuir* **1999**, *15*, 7534.

(9) Bonn, D.; Tanaka, H.; Kellay, H.; Wegdam, G.; Meunier, J. *Europhys. Lett.* **1998**, *45*, 52.

(10) Ruzicka, B.; Zulian, L.; Ruocco, G. *Langmuir* **2006**, *22*, 1106.

(11) Porion, P.; Faugere, A. M.; Lecolier, E.; Gherardi, B.; Delville, A. *J. Phys. Chem. B* **1998**, *102*, 3477.

(12) Porion, P.; Al Mukhtar, M.; Meyer, S.; Faugere, A. M.; van der Maarel, J. R. C.; Delville, A. *J. Phys. Chem. B* **2001**, *105*, 10505.

(13) Porion, P.; Al Mukhtar, M.; Faugere, A. M.; Delville, A. *J. Phys. Chem. B* **2004**, *108*, 10825.

(14) Jaccard, G.; Wimperis, S.; Bodenhausen, G. *J. Chem. Phys.* **1986**, *85*, 6282.

(15) Chung, C.; Wimperis, S. *Mol. Phys.* **1992**, *76*, 47.

(16) Tsoref, L.; Eliav, U.; Navon, G. *J. Chem. Phys.* **1996**, *104*, 3463.

(17) Lykos, C. N. *Phys. Rep.* **2001**, *348*, 267.

(18) Hubbard, P. S. *J. Chem. Phys.* **1970**, *53*, 985.

(19) Bull, T. E. *J. Magn. Reson.* **1972**, *8*, 344.

(20) Ernst, R. R.; Bodenhausen, G.; and Wokaun, A. *Principles of Nuclear Magnetic Resonance in One and Two Dimensions*; Oxford University Press: Oxford (1987).

(21) Muller, N.; Bodenhausen, G.; Wuthrich, K.; Ernst, R. R. *J. Magn. Reson.* **1985**, *57*, 531; Rance, M.; Wright, P. E. *Chem. Phys. Lett.* **1986**, *124*, 572.

(22) Thompson, D. W.; Butterworth, J. T. *J. Colloid Interface Sci.* **1991**, *151*, 236.

(23) Mourchid, A.; Levitz, P. *Phys. Rev. E* **1998**, *57*, R4887.

(24) Nicolai, T.; Cocard, S. *J. Colloid Interface Sci.* **2001**, *69*, 031404.

(25) Abou, B.; Bonn, D.; Meunier, J. *Phys. Rev. E* **2001**, *64*, 021510.

(26) Gili, T. Ph.D. Thesis, 2005.

(27) Jeener, J.; Meier, B. H.; Bachman, P.; Ernst, R. R. *J. Chem. Phys.* **1979**, *71*, 4546.